

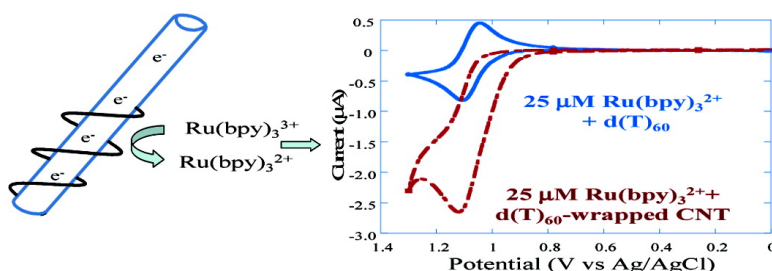
Communication

Electrocatalytic Oxidation of DNA-Wrapped Carbon Nanotubes

Mary E. Napier, Dominic O. Hull, and H. Holden Thorp

J. Am. Chem. Soc., **2005**, 127 (34), 11952-11953 • DOI: 10.1021/ja054162c • Publication Date (Web): 06 August 2005

Downloaded from <http://pubs.acs.org> on March 25, 2009



More About This Article

Additional resources and features associated with this article are available within the HTML version:

- Supporting Information
- Links to the 5 articles that cite this article, as of the time of this article download
- Access to high resolution figures
- Links to articles and content related to this article
- Copyright permission to reproduce figures and/or text from this article

[View the Full Text HTML](#)



ACS Publications
 High quality. High impact.

Electrocatalytic Oxidation of DNA-Wrapped Carbon Nanotubes

Mary E. Napier, Dominic O. Hull, and H. Holden Thorp*

Department of Chemistry, University of North Carolina, Chapel Hill, North Carolina 27599-3290

Received June 23, 2005; E-mail: holden@unc.edu

The electrical properties of single-walled carbon nanotubes (CNTs) are of intense interest due to applications in nanoelectronics.^{1–10} However, poor solubility in both aqueous and non-aqueous solvents has precluded the study of CNTs using modern, solution-based electrochemical techniques. Zheng et al. have recently discovered that sonication of DNA with CNTs is extremely effective at dispersing the nanotubes in aqueous solutions.^{1–3} One-electron oxidation of the solubilized CNTs can be effected by oxidants, such as KMnO_4 and K_2IrCl_6 ; the resulting oxidized CNTs can be fully re-reduced by reductants, such as NaBH_4 and $\text{Na}_2\text{S}_2\text{O}_4$.¹ On the basis of redox titration experiments, the density of reducing equivalents was calculated to be 0.2–0.4 electrons per 100 carbon atoms or approximately 1 electron per 5 nanometers of CNT.¹ The redox titration experiment suggests new applications using CNTs as a catalyst of redox reactions or as an electron donor in electrochemical reactions.

The kinetics and thermodynamics of guanine oxidation in complex nucleic acids are amenable to detailed study via the ability to observe electrocatalytic oxidation of guanine by $\text{Ru}(\text{bpy})_3^{2+}$ at indium tin oxide (ITO) electrodes in neutral solution. A critical characteristic of this system is the weak adsorption of the phosphate buffer anion to the electrode,¹¹ producing a high oxidative limit for ITO, rapid heterogeneous kinetics for $\text{Ru}(\text{bpy})_3^{2+}$, negligible adsorption of polyanions, and consequently, poor heterogeneous kinetics for direct oxidation of the polyanion. We report here that this ITO– $\text{Ru}(\text{bpy})_3^{2+}$ system provides a convenient platform for studying electrocatalytic oxidation of DNA-solubilized CNTs, which are surprisingly effective electron donors.

DNA dispersion of the CNTs was accomplished using a procedure similar to the one published by Zheng et al. (see Supporting Information).^{1–3} Specifically, CoMoCAT-process SWCNT purified single-walled carbon nanotubes were mixed with aqueous $\text{d}(\text{T})_{60}$ oligonucleotide and sonicated. The mixture was then centrifuged to remove the unsuspended CNTs. Following centrifugation, a substantial fraction of the oligonucleotide was still free in solution, not wrapped around a CNT. We found that separation of the free DNA from the DNA-wrapped CNT could be conveniently achieved using Y100 molecular weight cutoff filters. Ratios of DNA to CNT (mg/mL) of 2:1 or lower could be achieved with two passes through the Y100 filter. The CNT concentration was estimated using the optical absorption spectra and the finding of Diner and Zheng that 1 OD_{990 nm} is equivalent to approximately 13 μg of CNT material/mL, assuming a 1:1 mass ratio between the CNT and DNA derived from computer modeling.^{1,3} The oligonucleotide concentration was calculated using the 260 nm absorbance and the appropriate extinction coefficient.

Shown in Figure 1 are the cyclic voltammograms of 25 μM $\text{Ru}(\text{bpy})_3^{2+}$ and 25 μM $\text{Fe}(\text{dmb})_3^{2+}$ (inset) with either 1 μM $\text{d}(\text{T})_{60}$ oligonucleotide or $\text{d}(\text{T})_{60}$ -wrapped CNT at a concentration of 1 μM $\text{d}(\text{T})_{60}$ and 0.01 mg/mL CNT. Because the $\text{d}(\text{T})_{60}$ oligonucleotide contains no oxidizable guanines, there is no current enhancement for the samples that contain the metal complex and the oligonucle-

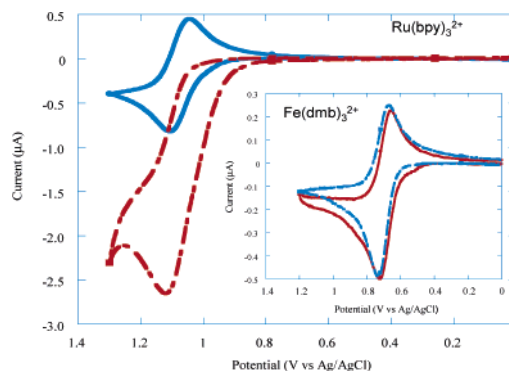


Figure 1. Electrochemical response for $\text{d}(\text{T})_{60}$ -wrapped CNT (red) and $\text{d}(\text{T})_{60}$ oligonucleotide (blue) in solution with either 25 μM $\text{Ru}(\text{bpy})_3^{2+}$ or 25 μM $\text{Fe}(\text{dmb})_3^{2+}$. The CNT concentration in these samples is 0.01 mg/mL and an oligonucleotide concentration of 0.018 mg/mL (1 μM). The scan rate is 25 mV/s. The current enhancement observed for the $\text{d}(\text{T})_{60}$ -wrapped CNT is due to oxidation of the CNT by electrogenerated $\text{Ru}(\text{III})$. No current enhancement was observed for the $\text{d}(\text{T})_{60}$ -wrapped CNT when $\text{Fe}(\text{dmb})_3^{2+}$ is the metal mediator at this concentration and the time scale of this experiment.

otide compared to cyclic voltammograms of the metal mediator alone (not shown). However, addition of the $\text{d}(\text{T})_{60}$ -wrapped CNT produces dramatic current enhancements *even when the metal complex catalyst is in a 25-fold excess compared to the oligonucleotide*. The current enhancement in the presence of $\text{d}(\text{T})_{60}$ -wrapped CNT is due to oxidation of the CNT by electrogenerated $\text{Ru}(\text{III})$ and subsequent recycling of the metal complex redox reaction. No current enhancement was observed for the $\text{d}(\text{T})_{60}$ -wrapped CNT with $\text{Fe}(\text{dmb})_3^{2+}$, suggesting that the rate of electron transfer is significantly reduced at this lower potential. At higher CNT concentrations, detectable catalytic current could be observed for $\text{Fe}(\text{dmb})_3^{2+}$, consistent with the potentials estimated from the redox titration experiment performed by Zheng and Diner.¹ It is very important to note that no oxidation current was observed for the wrapped CNT in the absence of metal complex, which is consistent with our observations on other oxidizable polyanions.¹¹ To our knowledge, this is the first observation of electrocatalytic oxidation of a CNT in fluid solution. As with DNA, relatively low quantities of CNT are required to obtain this signal; however, the absolute amount of wrapped CNT needed to induce current enhancement is much smaller than for DNA, even for sequences containing many guanine bases. Similar results were observed under high salt conditions (700 mM NaCl), suggesting that the extent of mediator binding is not playing a large role in the electron-transfer kinetics.¹²

Figure 2A shows the chronoamperometric (CA) response for $\text{Ru}(\text{bpy})_3^{2+}$ -mediated oxidation of $\text{d}(\text{T})_{60}$ -wrapped CNT in 0.1 M sodium phosphate buffer at pH 7. The plot of the current in the presence of CNT (i_{cat}) divided by the response in the absence of CNT (i_{d}) versus $t^{1/2}$ for three different concentrations of carbon nanotubes shows a biphasic response. For each curve, there are two linear regimes, an early, fast regime and a slower regime at

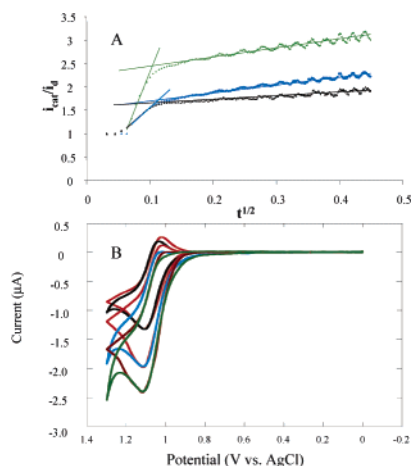
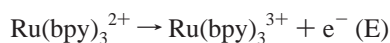


Figure 2. (A) Ratio of the CA traces obtained in the presence of CNT (i_{cat}) and in the absence of CNT (i_d) as a function of the square root of the time. The entire time trace is shown for 0.02 mg/mL of CNT (green), 0.01 mg/mL of CNT (blue), and 0.005 mg/mL of CNT (black). The solid lines are the linear fits to the early, fast phase and the later, slower phase. The slope of the lines fit to the data is equal to $(\pi k' C_z^*)^{1/2}$. (B) Cyclic voltammograms of d(T)₆₀-wrapped CNT with 25 μM Ru(bpy)₃²⁺ in 0.1 M sodium phosphate, pH = 7, showing the experimental data and simulations. All of the simulations are in red, and the experimental data are as follows: 0.005 mg/mL of CNT (black), 0.01 mg/mL of CNT (blue), and 0.02 mg/mL of CNT (green).

longer times. Similar responses have been previously observed with guanine-containing DNA, and the two regimes were interpreted as two phases of the electrocatalytic reaction.¹² The apparent second-order rate constants were determined from the slope of the best fit lines at the early and late times with slopes equal to $(\pi k' C_z^*)^{1/2}$.¹³ The rate constants (k') obtained were calculated using a concentration of reducing equivalents (C_z^*) derived from estimates by Zheng and Diner of an average CNT length of 140 nm and a number of redox-active sites equal to 1 per 5 nm.^{1–3} The rate constants obtained from the best fits to the data do not exhibit any systematic dependence on the carbon nanotube concentration, as expected. The fast phase exhibits an average rate constant of $6 \times 10^6 \text{ M}^{-1} \text{ s}^{-1}$, and the slow phase exhibits an average rate constant of $3.5 \times 10^4 \text{ M}^{-1} \text{ s}^{-1}$; note again that these rate constants are expressed in terms of 5 nm reducing equivalents, not for the whole CNT.

The rate constants derived from the chronoamperometric responses could be used to develop digital simulations of the cyclic voltammetry collected for the same CNT concentrations. The experimental data and the simulated curves for the Ru(bpy)₃²⁺-mediated CNT oxidation are shown in Figure 2B. To simulate the electrocatalytic signal, an EC' mechanism in the following form was employed:



In contrast to simulations of DNA oxidation, 10 successive C' reactions were required to account for the observed signal. The

number of C' reactions needed was determined systematically by successive testing of the addition of each new C' reaction at various homogeneous rate constants until the simulated electrocatalytic signal was similar to the experimental signal. The rate constants for the first homogeneous reaction (C') determined by simulating the data ranged from 3.8 to $5 \times 10^6 \text{ M}^{-1} \text{ s}^{-1}$, in excellent agreement with the rate constants derived from the fast portion of the CA trace. The rate constants that describe the later reaction steps are very similar to the rate constants derived from the slower portions of the CA trace. The later reactions are extremely important for achieving a good fit to the experimental data; representative calculated voltammograms with fewer following reactions are given in Supporting Information. The extensive follow-up chemistry likely results from reactions of the oxidized CNT with phosphate, water at neutral pH, and electrogenerated Ru(III) to produce oxidized carbon products similar to those observed in homogeneous reactions of CNTs with oxidants, such as potassium permanganate or nitric acid.^{4,9}

The voltammetric response shown in Figure 1 appears to be similar to that expected for a pseudo-first-order excess of reductant,¹³ yet the CNT concentration is far below that of the Ru(bpy)₃²⁺ catalyst; note that the absolute CNT concentration in Figure 1 is 0.65 μM . This effect arises from the multielectron nature of the oxidation, which arises both from multiple electron donor sites in the CNT¹ as well as the over oxidation of each site (by 10 electrons in these early simulations). The high absolute rate constants likely also point to a role for electronic delocalization along the CNT; the fractions used here are mostly semiconducting with some metallic CNTs.¹ The convenience of the Ru(bpy)₃²⁺-ITO system should allow for detailed study of these properties and a rigorous description of the CNT oxidation reaction.

Acknowledgment. The research was supported by Clinical Micro Sensors Inc. Helpful discussions with Professor T. J. Meyer are gratefully acknowledged.

Supporting Information Available: Detailed explanation of experimental procedures, as well as all of the rate constants derived from the simulations. A complete list of authors for ref 2 is also there. This material is available free of charge via the Internet at <http://pubs.acs.org>.

References

- Zheng, M.; Diner, B. A. *J. Am. Chem. Soc.* **2004**, *126*, 15490–15494.
- Zheng, M. et al. *Science* **2003**, *302*, 1545–1548.
- Zheng, M.; Jagota, A.; Semke, E. D.; Diner, B. A.; McLean, R. S.; Lustig, S. R.; Richardson, R. E.; Tassi, N. G. *Nat. Mater.* **2003**, *2*, 338–342.
- Katz, E.; Willner, I. *ChemPhysChem* **2004**, *5*, 1084–1104.
- O'Connell, M. J.; Boul, P.; Ericson, L. M.; Huffman, C.; Wang, Y.; Haroz, E.; Kuper, C.; Tour, J.; Ausman, K.; Smalley, R. E. *Chem. Phys. Lett.* **2001**, *342*, 265–271.
- Colbert, D. T.; Smalley, R. E. *Trends Biotechnol.* **1999**, *17*, 46–50.
- White, C. T.; Mintmire, J. W. *J. Phys. Chem. B* **2005**, *109*, 52–65.
- Baughman, R. H.; Zakhidov, A. V.; de Heer, W. A. *Science* **2002**, *297*, 787–792.
- Lin, Y.; Taylor, S.; Huaping, L.; Fernando, A. S.; Qu, L.; Wang, W.; Gu, L.; Zhou, B.; Sun, Y.-P. *J. Mater. Chem.* **2004**, *14*, 527–541.
- Kohli, P.; Wirtz, M.; Martin, C. R. *Electroanalysis* **2004**, *16*, 9–18.
- Armistead, P. M.; Thorp, H. H. *Anal. Chem.* **2000**, *72*, 3764–3770.
- Sistare, M. F.; Holmberg, R. C.; Thorp, H. H. *J. Phys. Chem. B* **1999**, *103*, 10718–10728.
- Bard, A. J.; Faulkner, L. R. *Electrochemical Methods*; John Wiley and Sons: New York, 1980; Chapter 11, pp 456–457.

JA054162C